Electronic Supporting Information

Suitability of alkyne donor-π- donor-π-donor scaffolds for electrofluorochromic and electrochromic use

Monika Wałęsa-Chorab,[1,2*] Kacper Muras,[2] Heather L. Filiatrault,[1] and W.G. Skene[1*]

[1]Laboratoire de caractérisation photophysique des matériaux conjugués Département de Chimie, Campus MIL, Université de Montréal, CP 6128, succ. Centre-ville, Montréal, Québec, Canada H3C 3J7

[2]Faculty of Chemistry, Adam Mickiewicz University in Poznań, Uniwersytetu Poznanskiego 8, 61-614 Poznań, Poland

Table of Contents

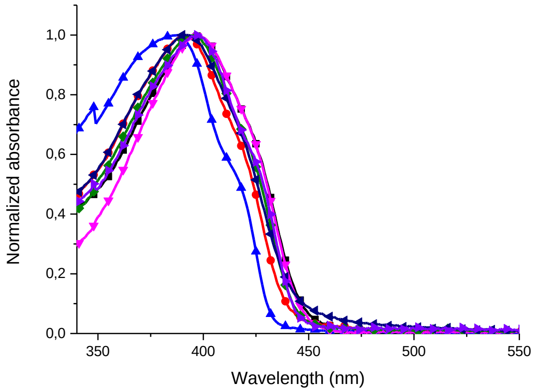

Figure S1. Normalized absorption spectra of **1** measured in hexane (▲), toluene (▶), THF (♦), ethanol (●), dichloromethane (■), acetone (▼) and acetonitrile (◀).

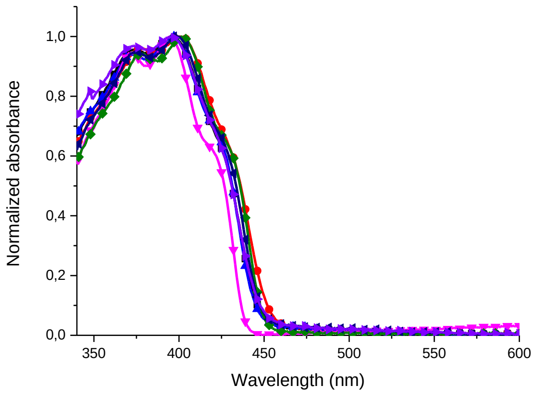

Figure S2. Normalized absorption spectra of **2** measured in hexane (▼), toluene (♦), THF (◀), ethanol (▲), dichloromethane (●), acetone (■) and acetonitrile (▶).

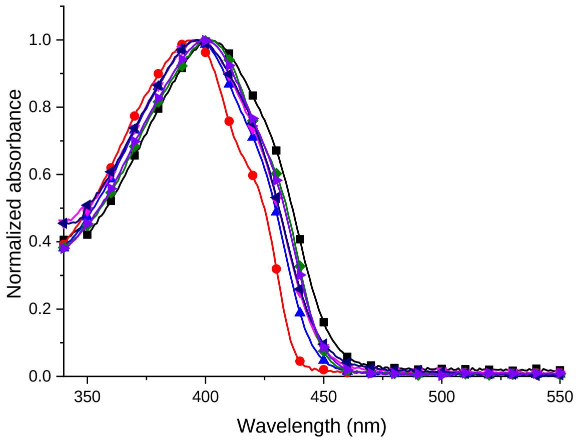

Figure S3.Normalized absorption spectra of **3** measured in hexane (●), toluene (♦), THF (▶), ethanol (▲), dichloromethane (■), acetone (▼) and acetonitrile (◀).

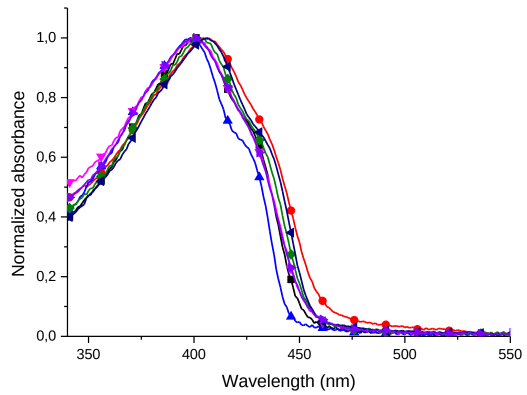

Figure S4. Normalized absorption spectra of **4** measured in hexane (▲), toluene (◀), THF (♦), ethanol (■), dichloromethane (●), acetone (▼) and acetonitrile (▶).

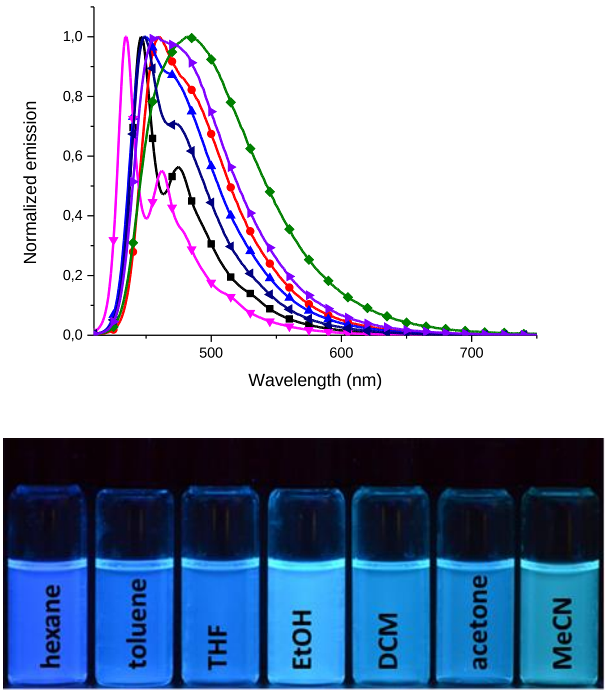

Figure S5. Top: normalized emission spectra of **2** measured in hexane (▼), toluene (■), THF (◀), ethanol (▲), dichloromethane (●), acetone (▶) and acetonitrile (♦). Bottom: photograph showing the fluorescence of **2** in different solvents.

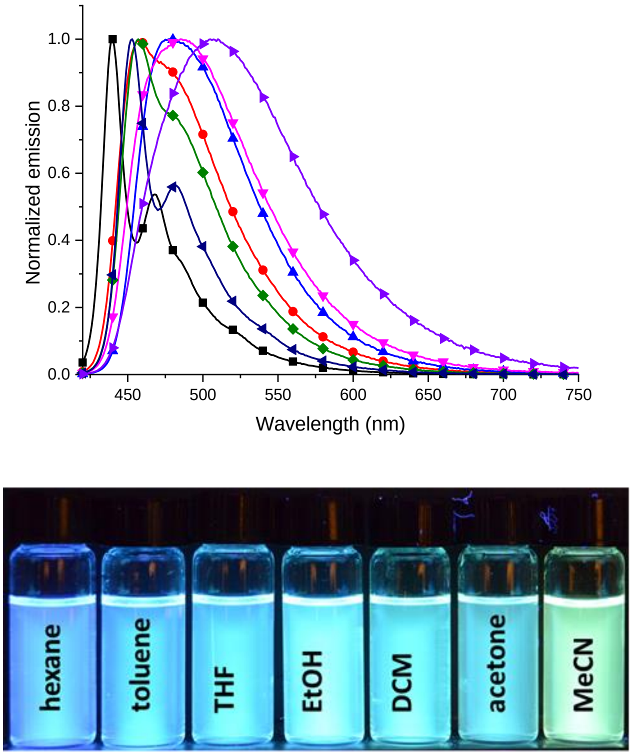

Figure S6. Top: normalized emission spectra of **4** measured in hexane (■), toluene (◀), THF (♦), ethanol (●), dichloromethane (▲), acetone (▼) and acetonitrile (▶). Bottom: photograph showing the fluorescence of **4** in different solvents.

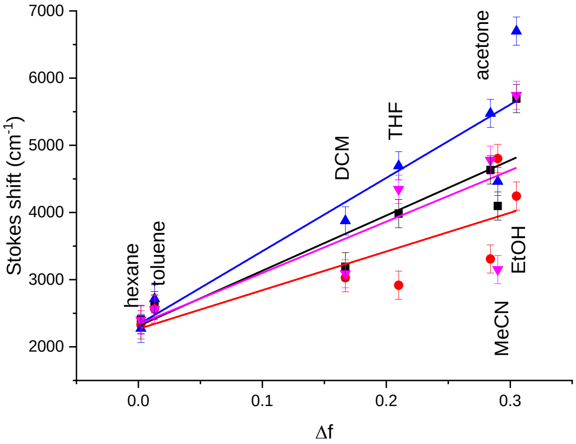

Figure S7. Stokes shift of **1** (■), **2** (●), **3** (▲), and **4** (▼) as a function of solvent orientation polarizability (Δf) for various solvents.

Table S1. Linear regression fitting parameters for Stokes shift as a function of solvent orientation polarizability (Δf) for various solvents.

	Intercept		**Slope**		**Statistics**
Compound	Value	Standard Error	Value	Standard Error	Adj. R-Square
1	2311	367	8219	1690	0.791
2	2267	385	5764	1772	0.615
3	2332	467	10914	2153	0.805
4	2337	589	7635	2713	0.536

Table S2. Linear regression fitting parameters for Stokes shift as a function of $E_T(30)$.

	Intercept		**Slope**		**Statistics**
Compound	Value	Standard Error	Value	Standard Error	Adj. R-Square
1	-4975	1030	227	27	0.935
2	-3114	1364	167	35	0.812
3	-7493	787	306	20	0.979
4	-5474	1059	242	27	0.939

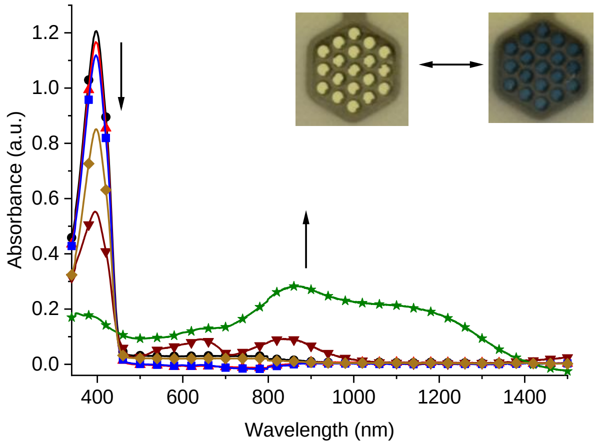

Figure S8. The spectroelectrochemistry of **1** in anhydrous and deaerated dichloromethane with TBAPF6 (0.1 M) as an electrolyte with applied potential 0 (●), 700 (▲), 800 (■), 900 (▼) and 1000 (★) mV followed by -500 (♦) mV held for 30 sec per potential. Inset: photographs of honeycomb electrode of the original (left) and the electrochemically oxidized (right) **1** by applying a potential of 1000 mV for 1 min.

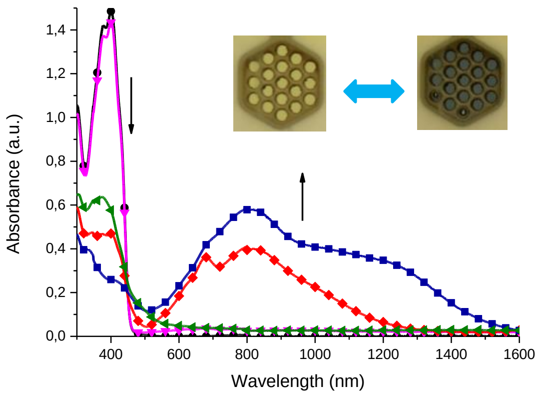

Figure S9. The spectroelectrochemistry of **2** in anhydrous and deaerated dichloromethane with TBAPF$_6$ (0.1 M) as an electrolyte with applied potentials of 0 (●), 800 (▼), 900 (♦), and 1000 (■) mV followed by -500 (◀) mV held for 30 sec per potential. Insert: photographs of original (left) and electrochemically oxidized (right) **2** by applying a potential of 1000 mV for 1 min.

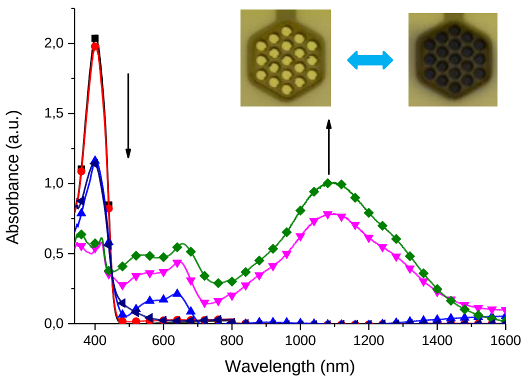

Figure S10.The spectroelectrochemistry of **3** in anhydrous and deaerated dichloromethane with TBAPF$_6$ (0.1 M) as an electrolyte with applied potentials of 0 (■), 700 (●), 800 (▲), 900 (▼), and 1000 (♦) mV followed by -500 (◀) mV held for 30 sec per potential. Insert: photographs of original (left) and electrochemically oxidized (right) **3** by applying a potential of 1000 mV for 1 min.

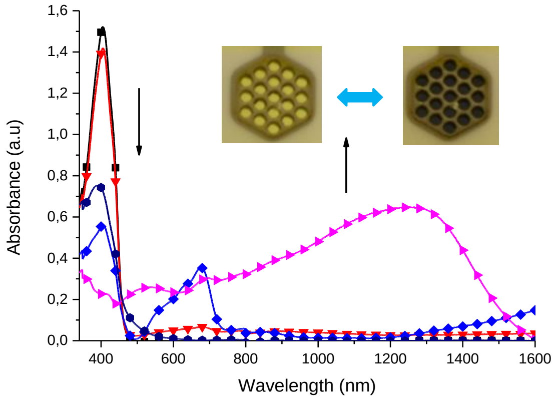

Figure S11. The spectroelectrochemistry of **4** in anhydrous and deaerated dichloromethane with $TBAPF_6$ (0.1 M) as an electrolyte with applied potentials of 0 (■), 800 (▼), 900 (♦), and 1000 (▶) mV followed by -500 (●) mV held for 30 sec per potential. Insert: photographs of original (left) and electrochemically oxidized (right) **4** by applying a potential of 1000 mV for 1 min.

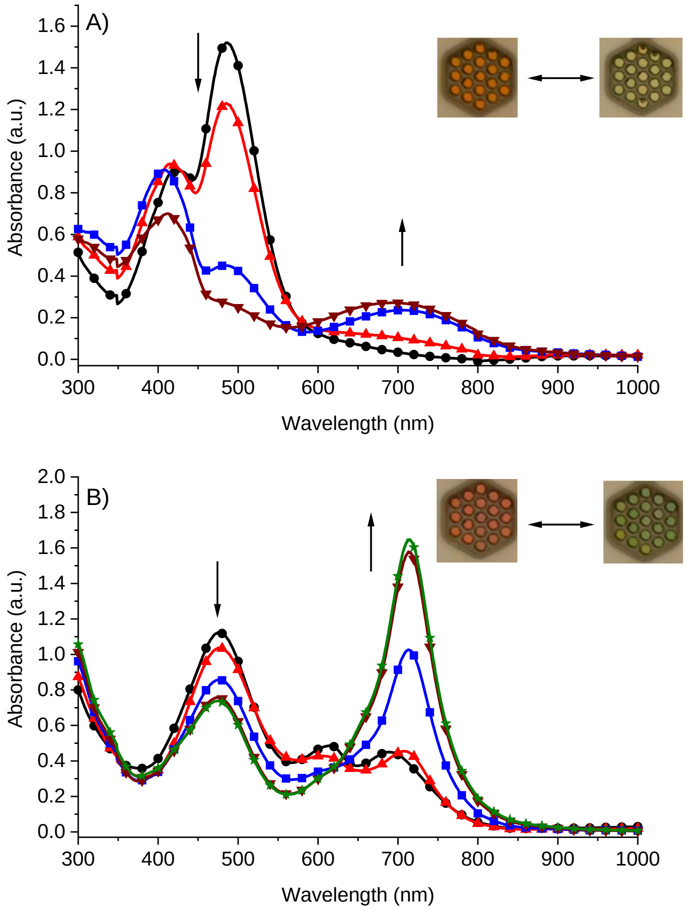

Figure S12. The spectroelectrochemistry of **5** in anhydrous and deaerated dichloromethane with $TBAPF_6$ (0.1 M) as an electrolyte with applied potential*:* A) 0 (●), 1200 (▲), 1300 (■), and 1400 (▼) mV; B) -300 (●), -400 (▲), -500 (■) -600 (▼), and -700 (★) mV held for 30 sec per potential. Inset: photographs of the honeycomb electrode of **5** A) original (left) and electrochemically oxidized (right) by applying a potential of 1400 mV for 1 min.; B) potential of -300 mV (left) and -700 mV applied for 1 min.

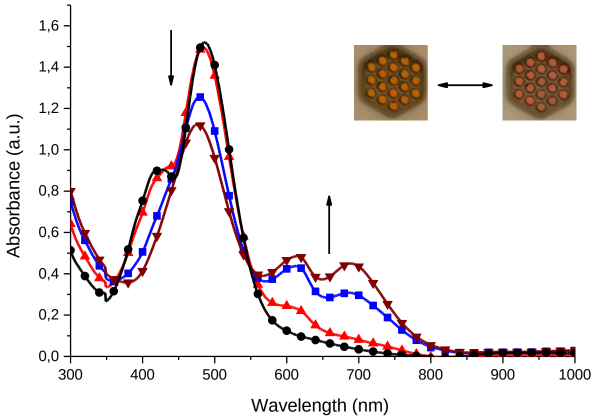

Figure S13. The spectroelectrochemistry of **5** in anhydrous and deaerated dichloromethane with 0.1 M $TBAPF_6$ as an electrolyte with applied potential 0 (●), -100 (▲), -200 (■) and -300 (▼) mV. Insert: photographs of original (left) and electrochemically reduced (right) **5** by applying a potential of -300 mV for 1 min.

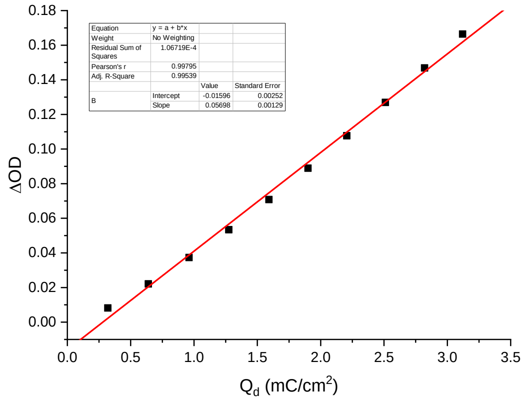

Figure S14. The change in optical density of **1** monitored at 730 nm as a function of charge density at +2.6 V.

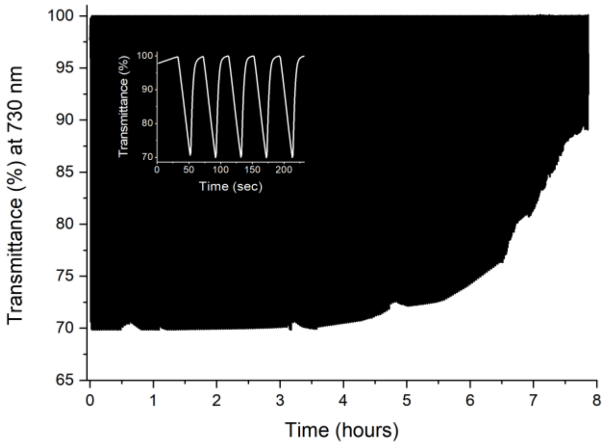

Figure S15. Baseline corrected change in percent transmittance of the electrochromic device prepared from **1** monitored at 730 nm with applied potential of 2.5 and -1.5 V switched at 20 s intervals during 8 hours of continuous operation. Inset: zoom of the first five switching cycles of applied potential.

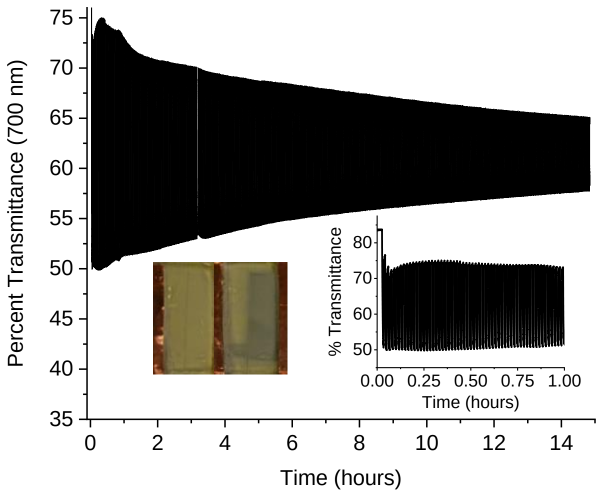

Figure S16. Change in percent transmittance of **2** monitored at 700 nm in an electrochromic device that was fabricated by spin coating and sealed under inert atmosphere and operating continuously for 15 hr. Inset: photographs of the neutral (left) and oxidized (middle) of electrochromic device and zoom of initial first hour of device operation (right).

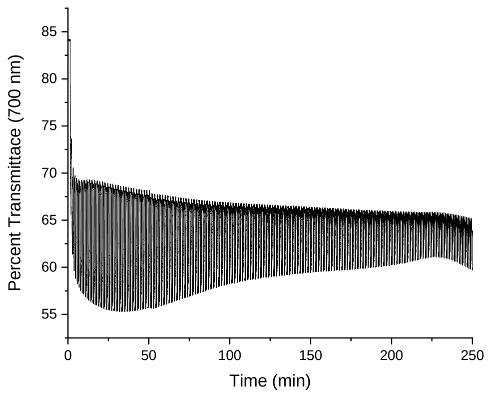

Figure S17. Change in transmittance of spray coated **2** (0.5 mg/mL) in an operating electrochromic device monitored at 700 nm when switching between applied potentials of 2.75 and -0.75 V at 30 s cycling speed.

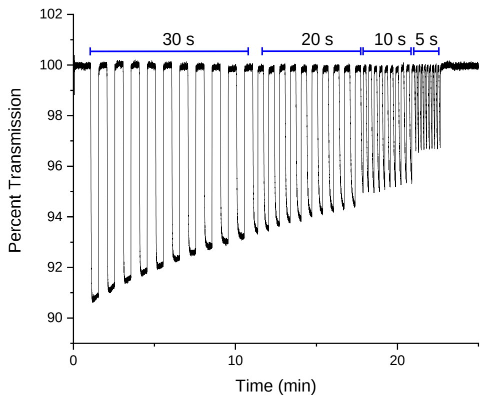

Figure S18. Baseline corrected change in percent transmittance of spin coated **2** on ITO coated glass in an operating electrochromic device monitored at 700 nm at different times of applied potential of 2.5 and -0.5 V.

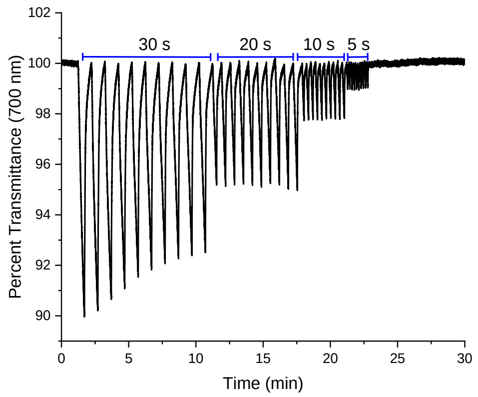

Figure S19. Baseline corrected change in percent transmittance of spin coated **2** on ITO coated PET in an operating electrochromic device monitored at 700 nm with different times of applied potential of 2.5 and -0.5 V.

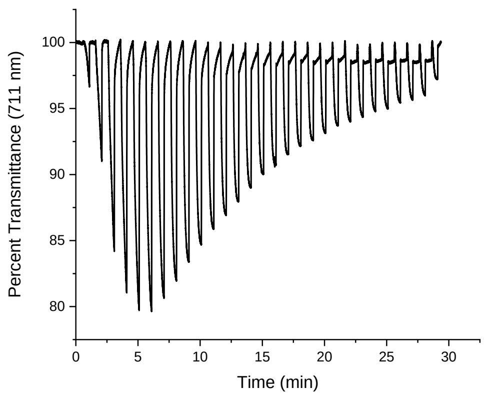

Figure S20. Baseline corrected change in percent transmittance of spin coated **3** in an electrochromic device monitored at 711 nm when switching the applied potential between 3 and -1 V at 30 s intervals.

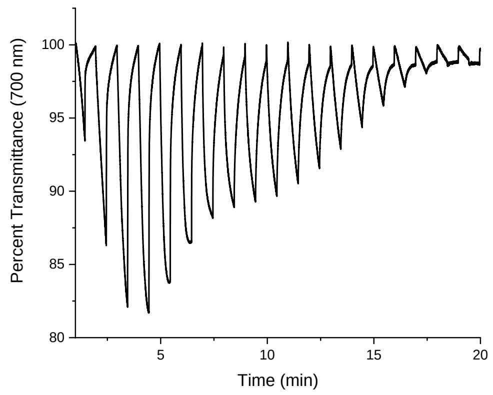

Figure S21. Baseline corrected change in percent transmittance of spin coated **4** (10 mg/mL) in an electrochromic device monitored at 700 nm when switching the applied potential of +2.9 and -1 V at 30 s intervals.

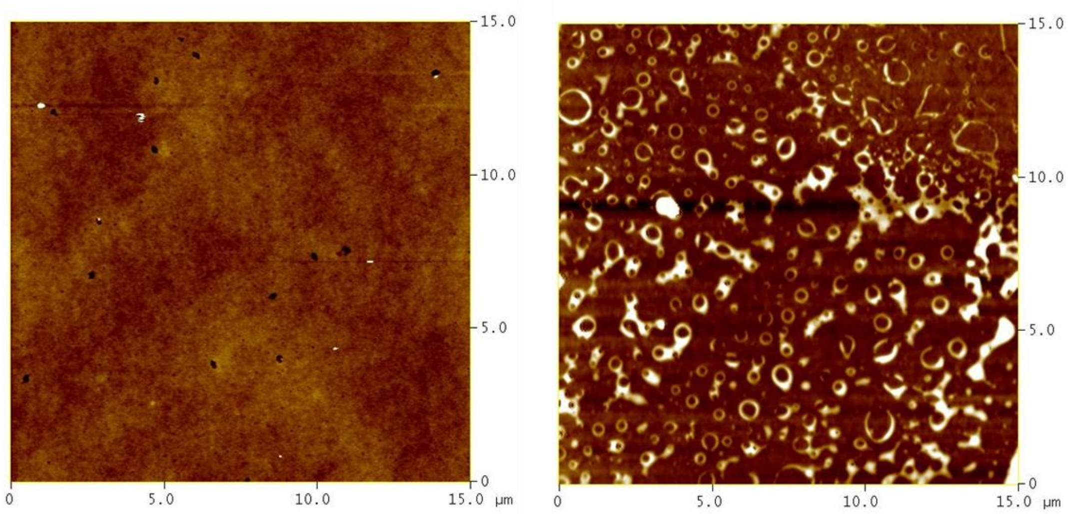

Figure S22. AFM images for surface roughness analyses of **2** spin coated (left) and spray coated (right) on ITO coated glass.

Table S3. RMS roughness of spin and spray coated films of **1** and **2**.

Sample	**Avg RMS Roughness 3 μm x 3 μm**	**Avg RMS Roughness 15 μm x 15 μm**	**RMS Roughness 50 μm x 50 μm**
2 Spin coated	0.7 ± 0.2 nm	0.7 ± 0.2 nm	2.2 nm
2 Spray coated	6.0 ± 4.5	15.1 ± 9.6 nm	26.1 nm
1 Spin coated	0.7 ± 0.1 nm	1.4 ± 0.8 nm	6.3 nm

Table S4. Average thickness by profilometry of spray coated alkyne layer in an electrochromic device.

Molecule	**Average Thickness (nm)**
1	71 ± 12
2	67 ± 19
3	67 ± 20
4	58 ± 19

Figure S23. Photograph of electrochromic device of **2** on ITO/PET curved around a beaker (radius=7 cm) with an applied potential of +2.5 V.

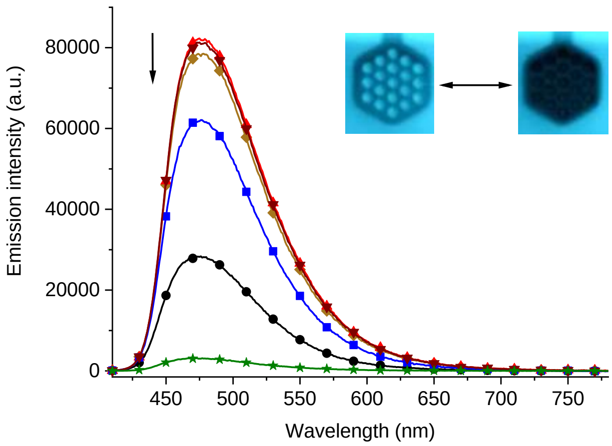

Figure S24. Fluorescence change of **1** in anhydrous and deaerated solution of dichloromethane with $TBAPF_6$ (0.1 M) when excited at 390 nm with applied potentials of 0 (●), 800 (▲), 900 (■), 1000 (▼) and 1100 (★) mV followed by −100 (♦) mV held for 30 sec per potential. Inset: photographs of the honeycomb electrode of the original (left) and electrochemically oxidized (right) **1** by applying a potential of 1000 mV for 1 min when irradiated with the handheld UV lamp (365 nm).

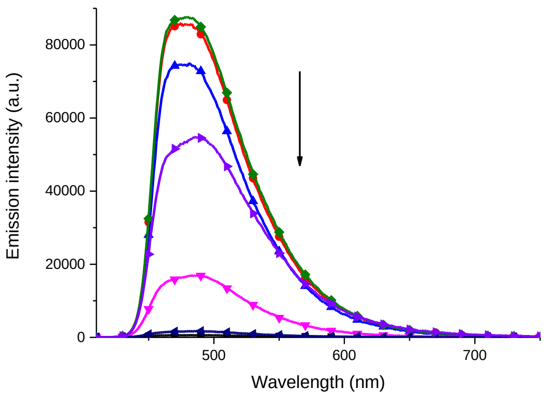

Figure S25. Fluorescence change of **2** in anhydrous and deaerated dichloromethane with $TBAPF_6$ (0.1 M) as an electrolyte when excited at 390 nm with applied potentials of 0 (♦), 700 (●), 800 (▲), 900 (◀), 1000 (▼), and 1100 (■) mV followed by −100 (▶) mV held for 30 sec per potential.

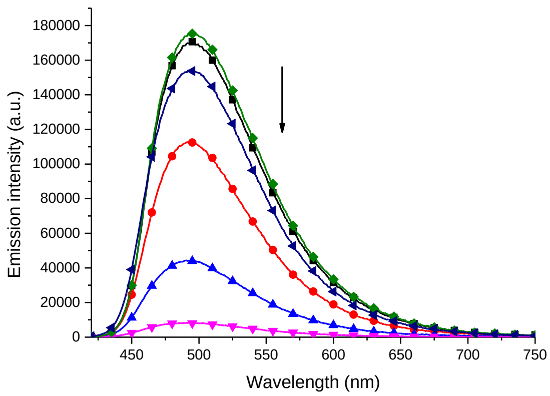

Figure S26. Fluorescence change of **3** in anhydrous and deaerated dichloromethane with $TBAPF_6$ (0.1 M) as an electrolyte when excited at 400 nm with applied potentials f 0 (♦), 700 (■), 800 (●), 900 (▲), and 1000 (▼) mV followed by −100 (◀) mV held for 30 sec per potential.

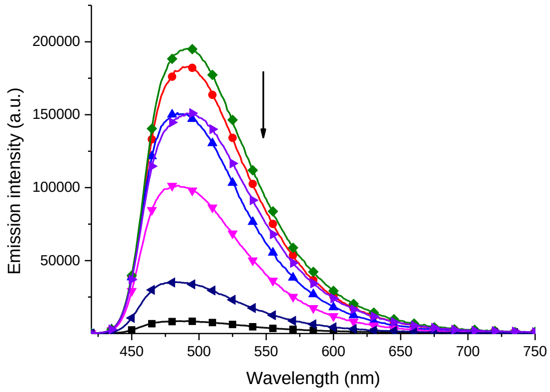

Figure S27. Fluorescence change of **4** in anhydrous and deaerated dichloromethane with $TBAPF_6$ (0.1 M) as an electrolyte when excited at 405 nm with applied potentials of 0 (♦), 700 (●), 800 (▲), 900 (▼), 1000 (◀), and 1100 (■) mV followed by −500 (▶) mV held for 30 sec per potential.

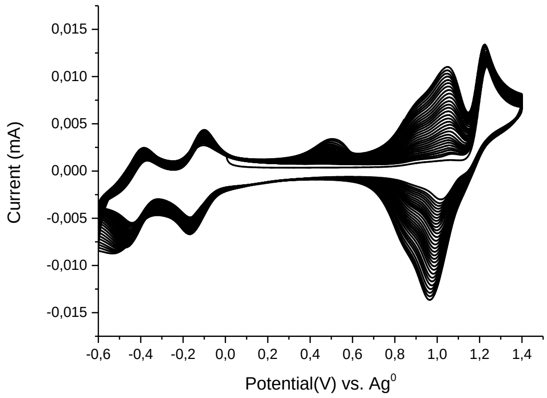

Figure S28. Cyclic voltammogram of **5** measured in DCM with $TBAPF_6$ (0.1 M) at 100 mV/sec.

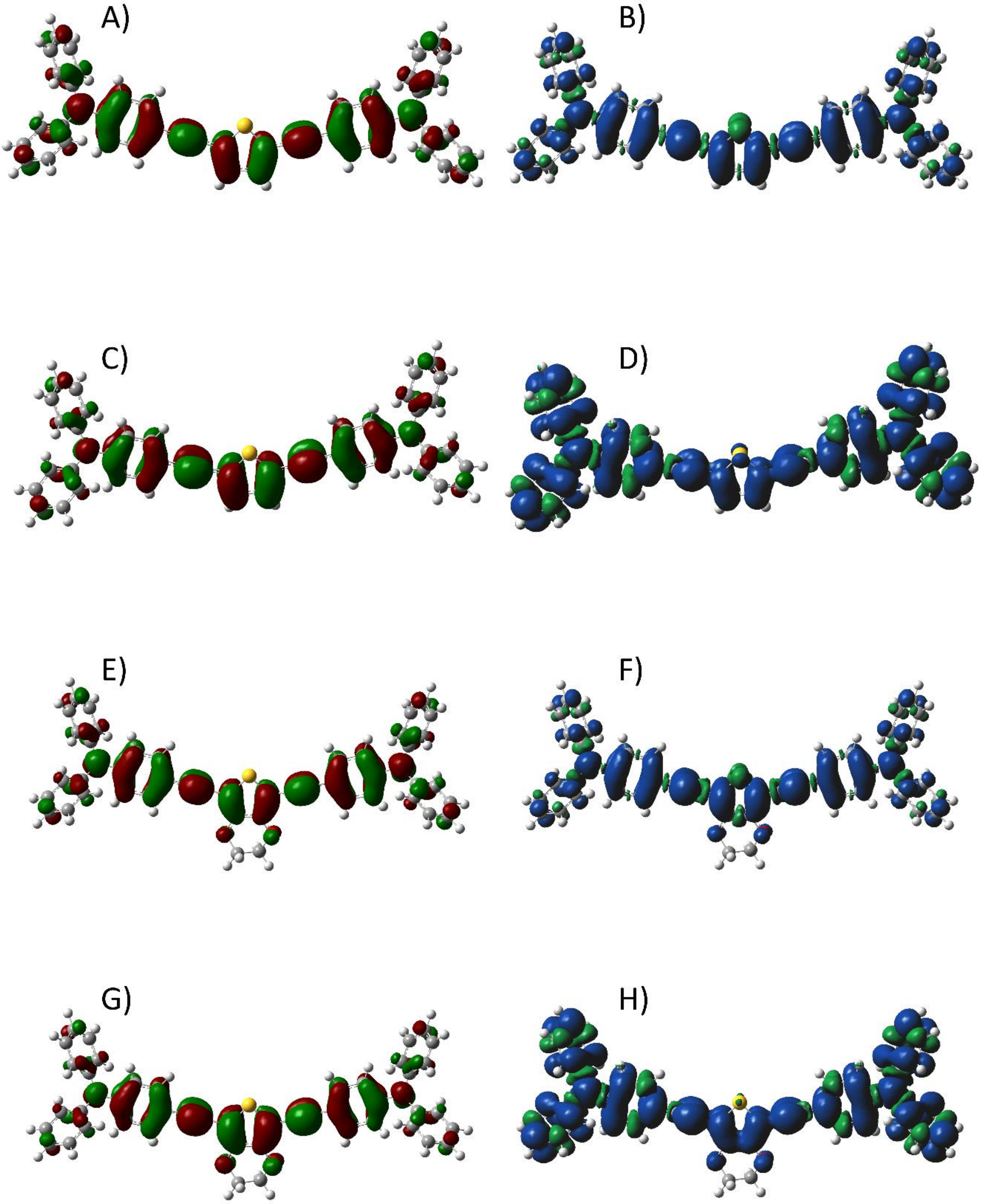

Figure S29. SOMO (left) and spin distribution (right) of the radical cation of **1** (A-B) and **2** (E-F) along with the bis(radical cation) of **1** (C-D) and **2** (G-H) calculated by B3LYP DFT with the 6-311+g(d,p) basis set.

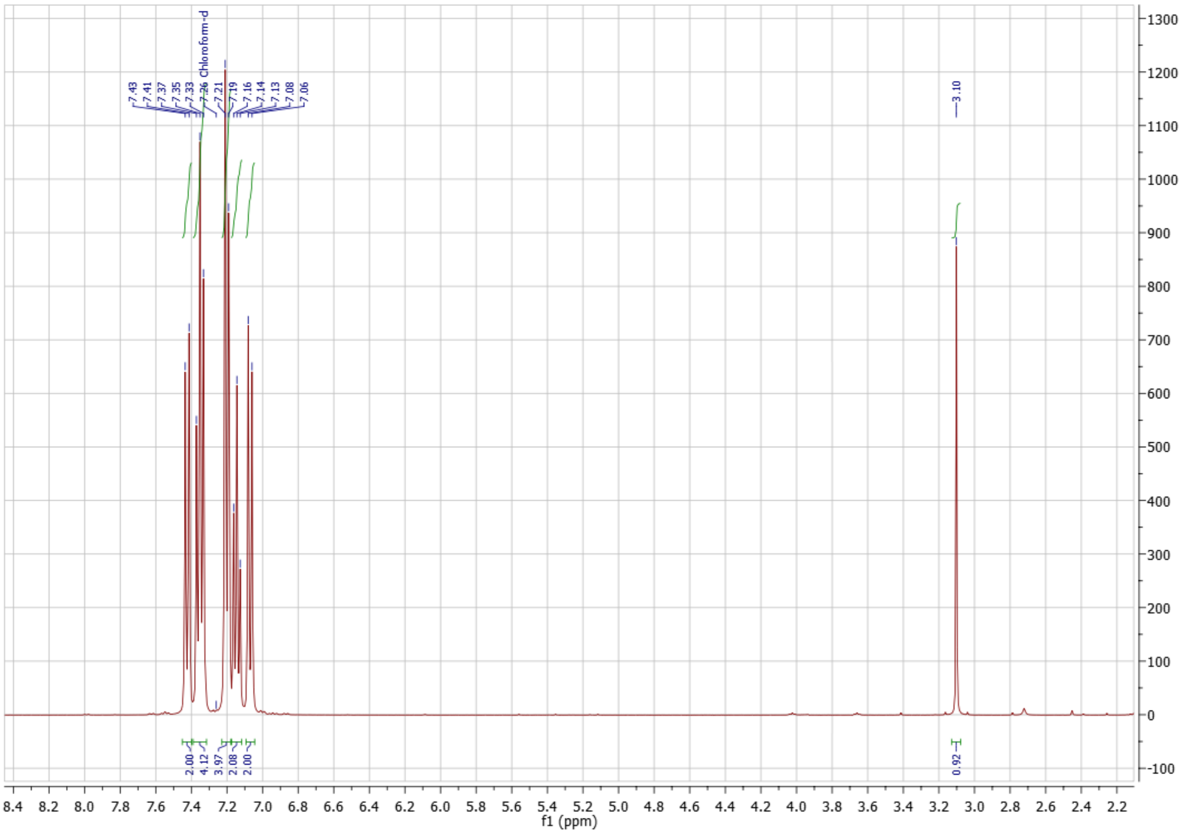

Figure S30.[1]H NMR of **A** in $CDCl_3$.

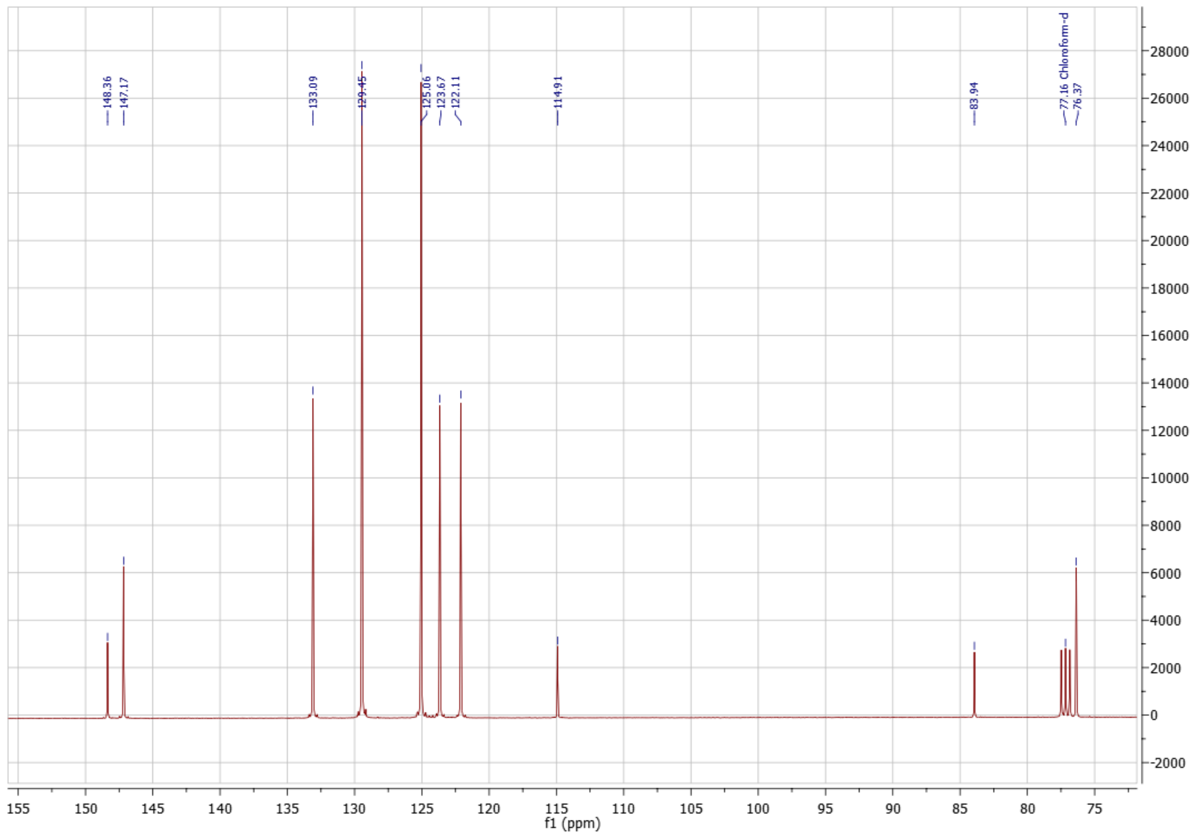

Figure S31. ^{13}C NMR spectra of **A** in $CDCl_3$.

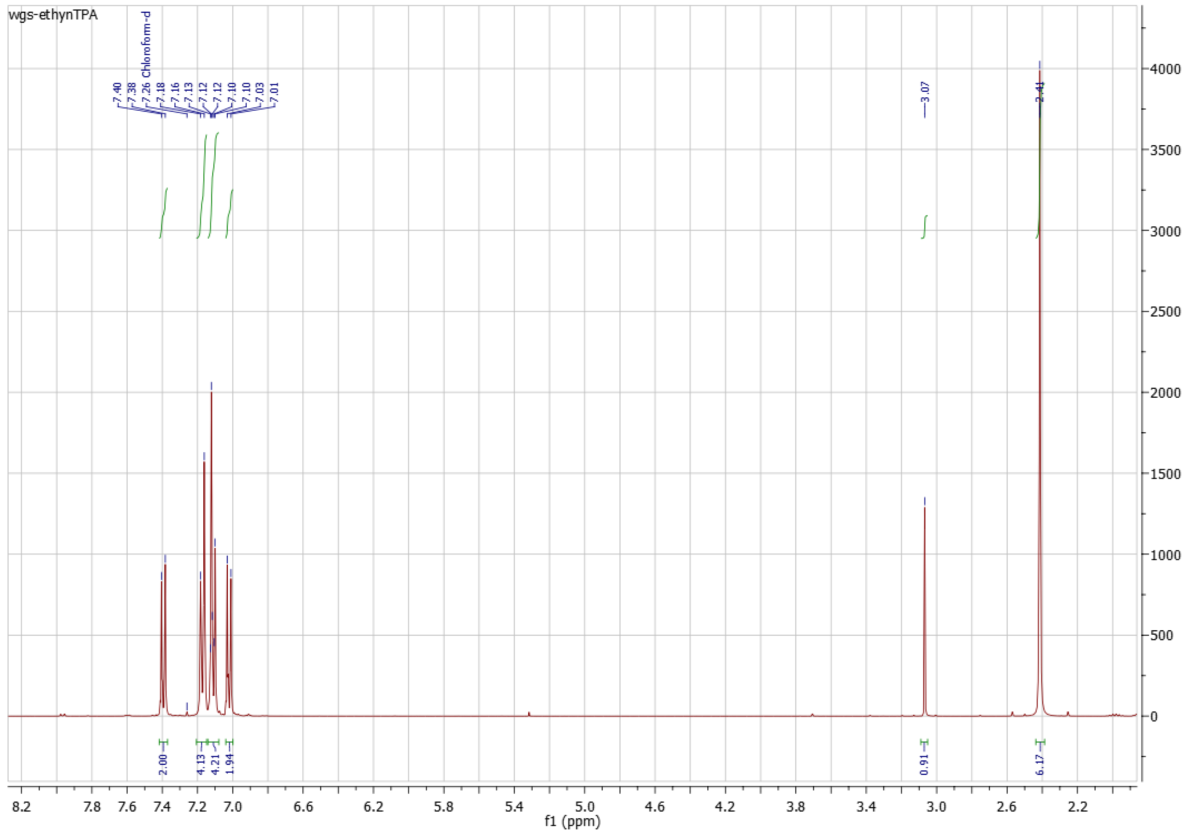

Figure S32. ^{1}H NMR spectra of **B** in $CDCl_3$.

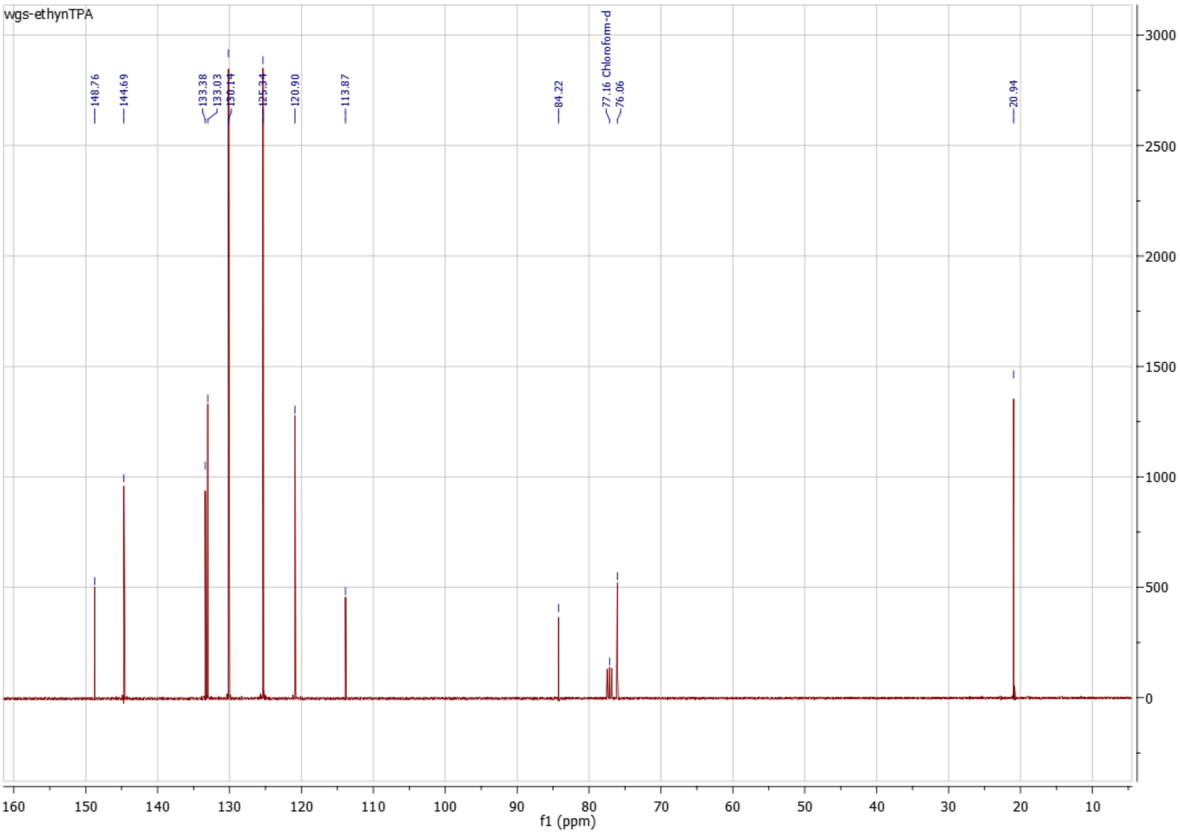

Figure S33. ^{13}C NMR spectra of **B** in $CDCl_3$.

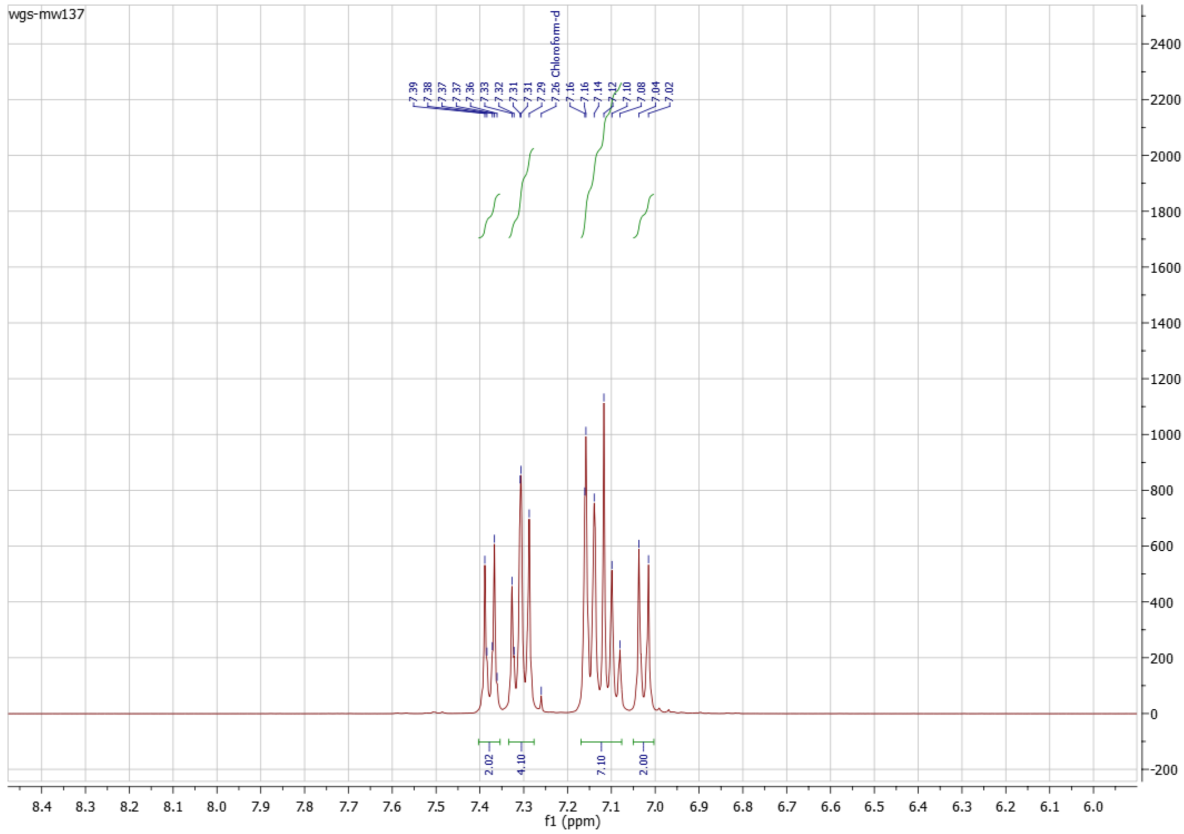

Figure S34. ^{1}H NMR spectra of **1** in $CDCl_3$.

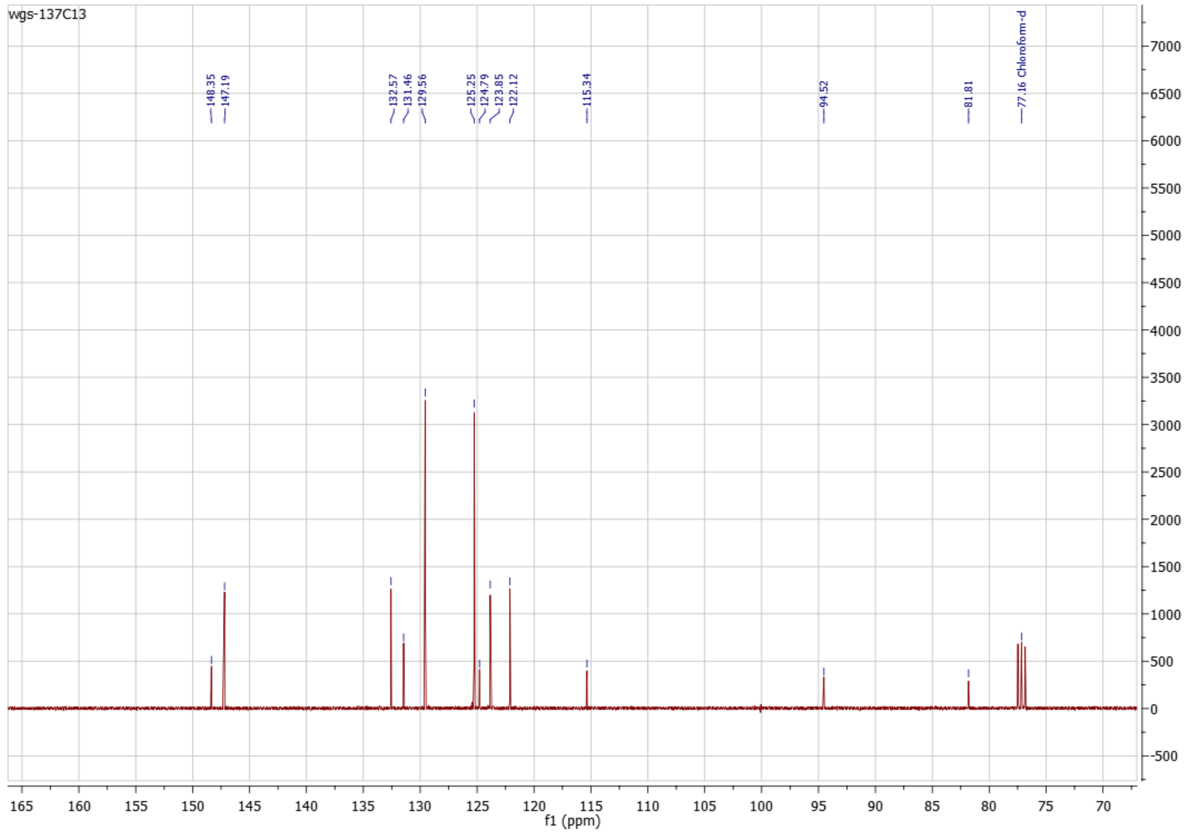

Figure S35. [13]C NMR spectra of **1** in $CDCl_3$.

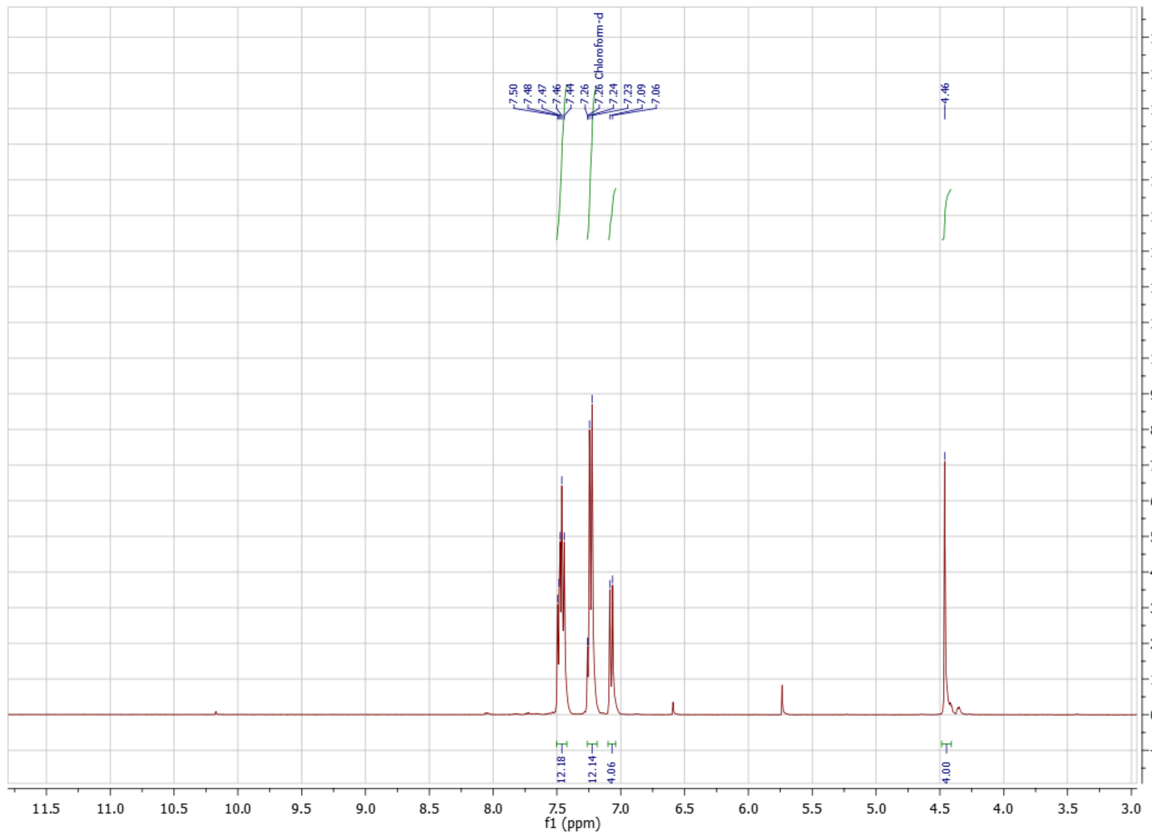

Figure S36. ^{1}H NMR spectra of **2** in $CDCl_3$.

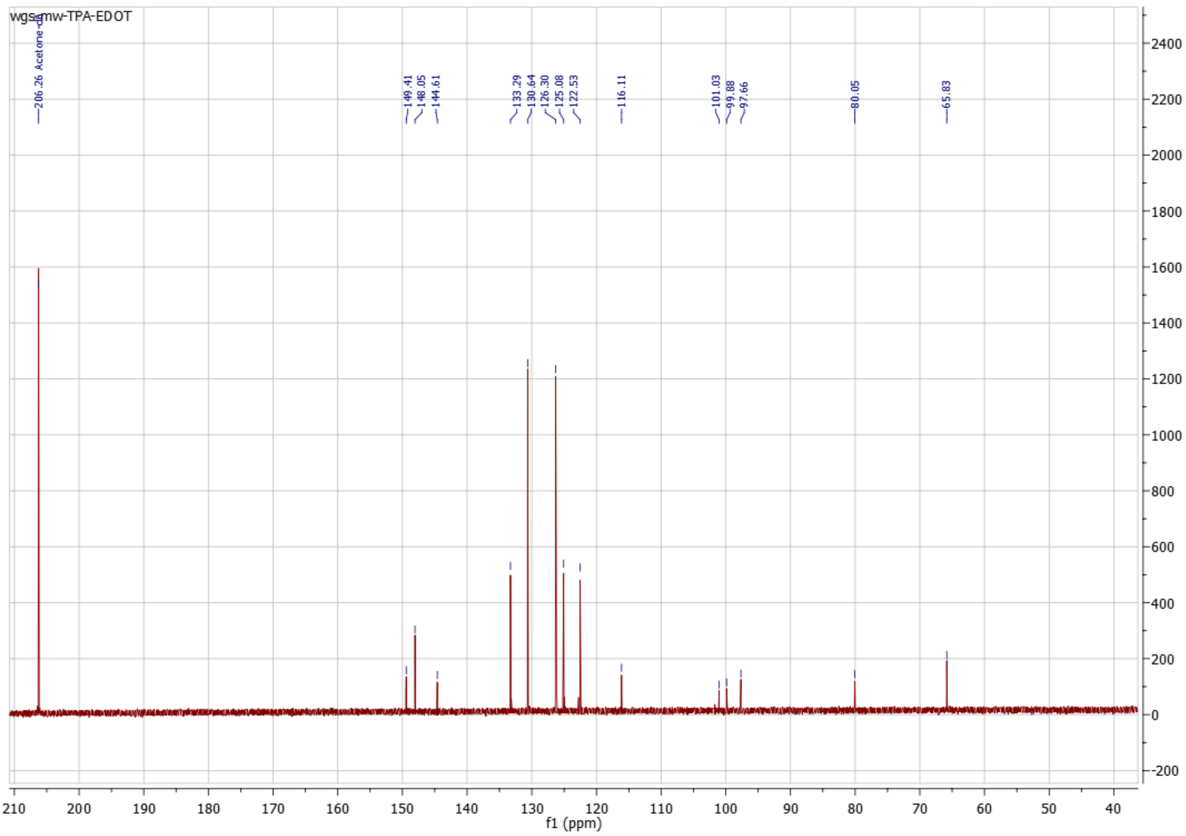

Figure S37. ^{13}C NMR spectra of **2** in acetone-d_6.

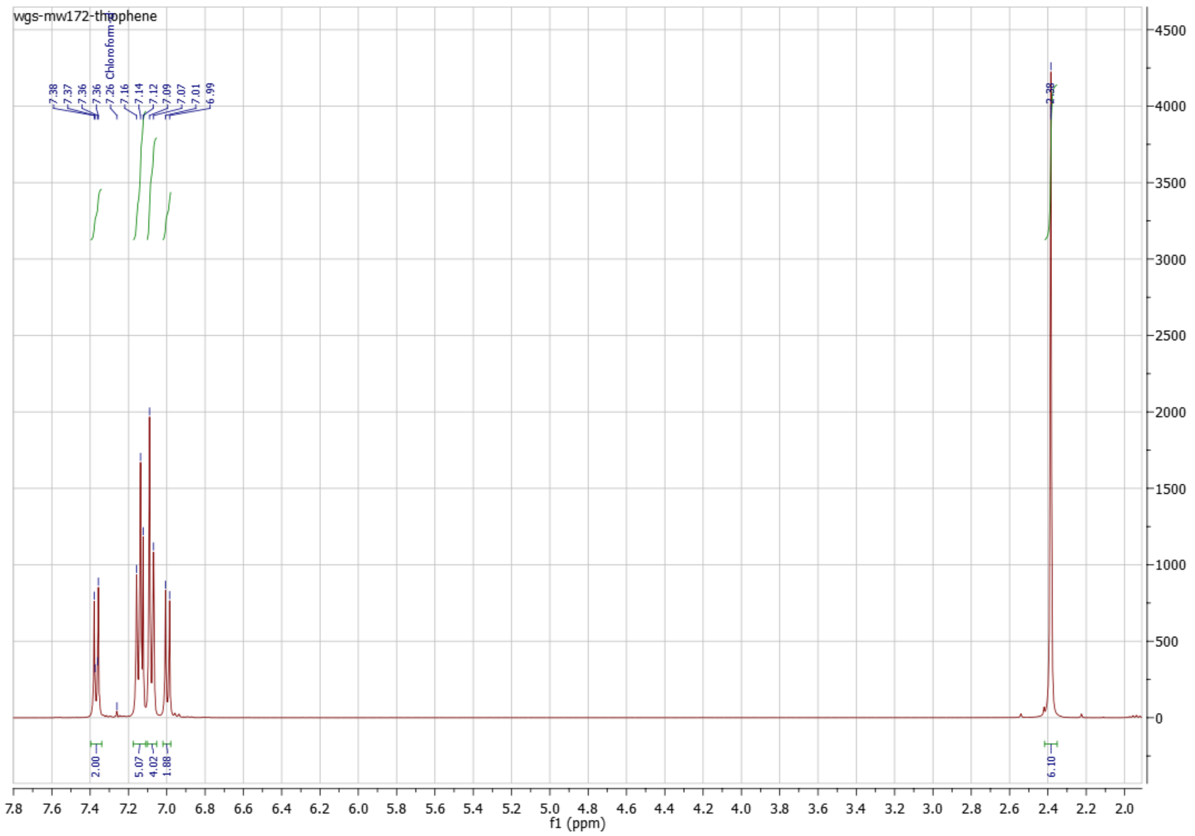

Figure S38. ^{1}H NMR spectra of **3** in $CDCl_3$.

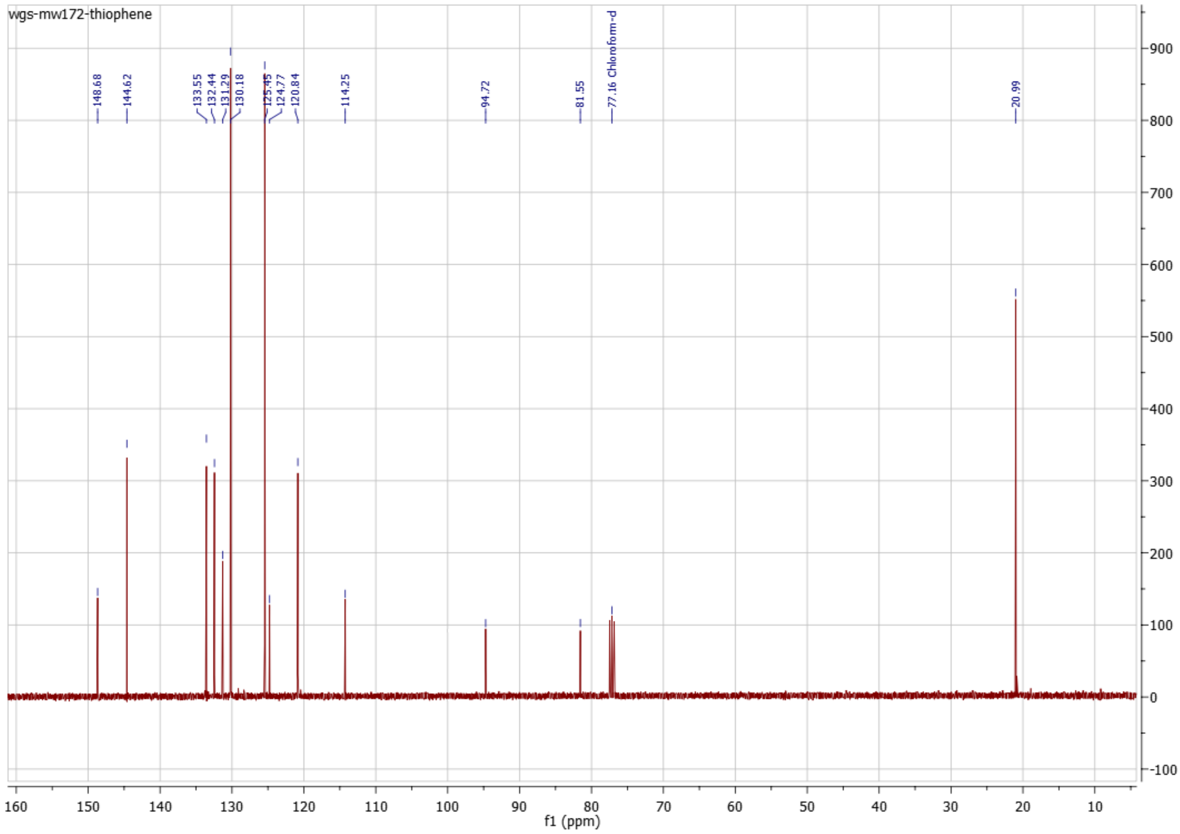

Figure S39. ^{13}C NMR spectra of **3** in $CDCl_3$.

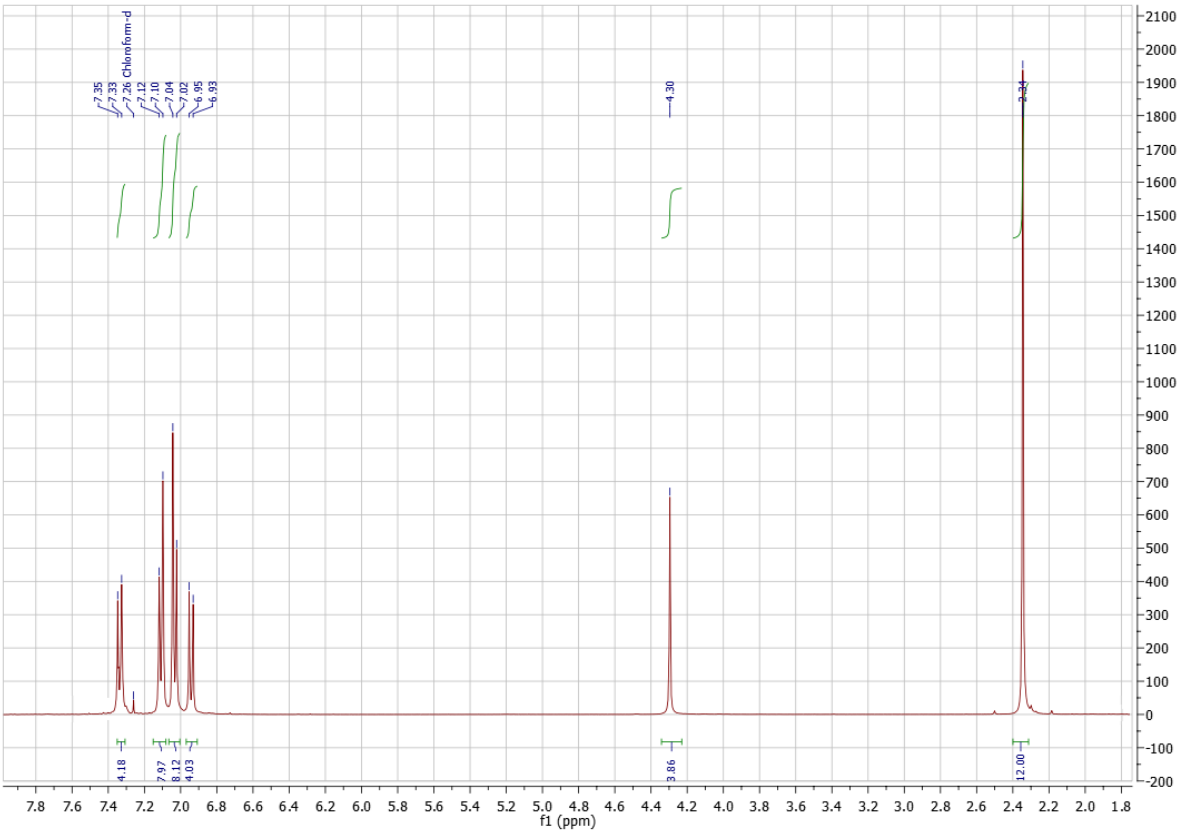

Figure S40. ^{1}H NMR spectra of **4** in $CDCl_3$.

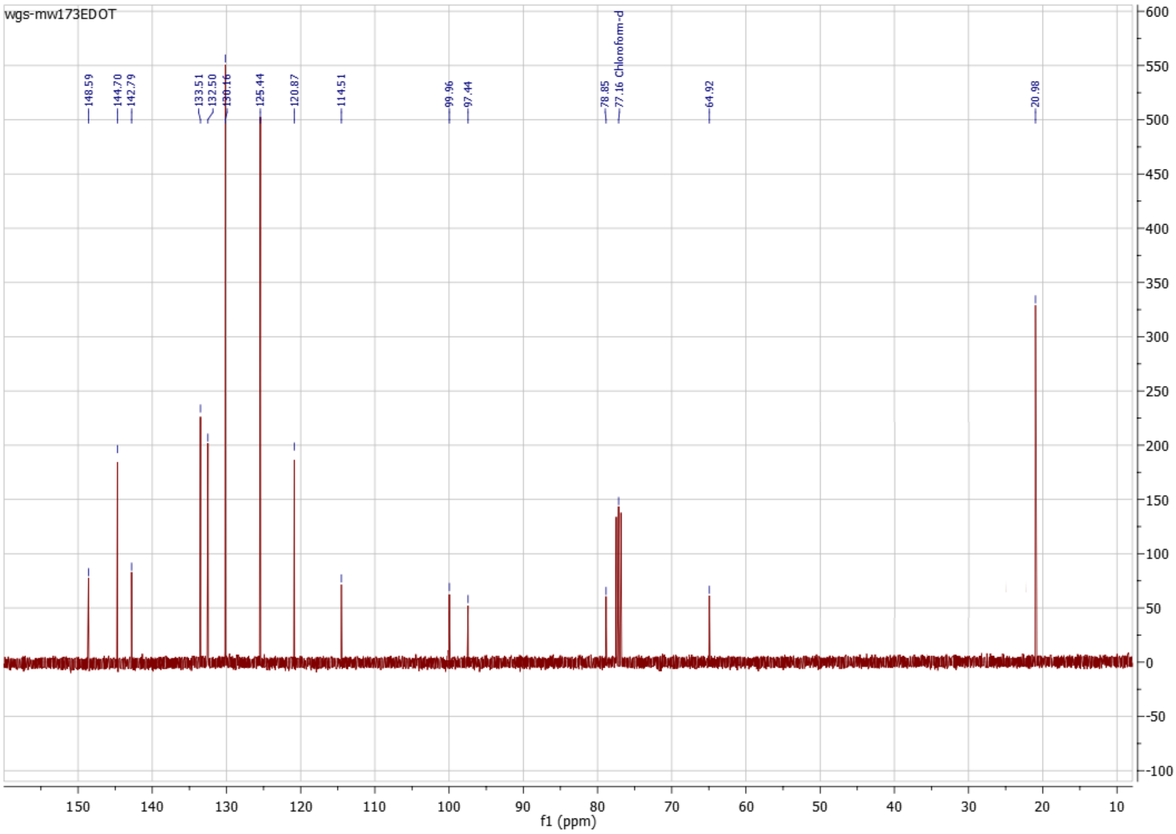

Figure S41. ^{13}C NMR spectra of **4** in $CDCl_3$.